Journal of Engineering Physics and Thermophysics, Vol. 79, No. 6, 2006

REVIEWS

NEW COMPOSITE SORBENTS OF WATER AND AMMONIA FOR CHEMICAL AND ADSORPTION HEAT PUMPS

Yu. I. Aristov[a] **and L. L. Vasiliev**[b]

UDC 621.575.9

New sorbents of water and ammonia — "salt in porous matrix" composites and "salt on fiber" composites — have been reviewed. The possibility of "constructing" the sorption properties of the composites at the nanophase level by varying their composition, the size of the host-matrix pores, and synthesis conditions has been shown. The application of the new materials in adsorption refrigerating devices has been considered.

Chemical and adsorption heat pumps (CHPs and AHPs) are considered alternatives of compression pumps, although examples of their commercial use are still few in number [1, 2]. The operation of CHPs is based on the reversible chemical reaction gas–solid body

$$A_g + B_{sol} \leftrightarrow (A{\cdot}B)_{sol} . \quad (1)$$

As the solid body B, one usually uses inorganic salts that form the complex A·B with the working fluid A: $B{\cdot}nH_2O$ hydrates with water, $B{\cdot}nNH_3$ ammoniates with ammonia, etc. The simplest CHP cycle includes two processes: the chemical reaction (1) with monovariant equilibrium (line 1 in Fig. 1) and the evaporation and condensation of a pure working fluid (line 2). Heat is absorbed in the evaporator at temperature T_e and is released in the condenser at temperature T_c, i.e., heat and cold are generated simultaneously. The cycle is activated by the external heat source which initiates the decomposition of the complex $(A{\cdot}B)_{sol}$ at pressure P_c and temperature T_d.

The first CHP was developed by Faraday in 1824 on the basis of the NH_3–AgCl working pair [3]. Although it is precisely CHPs that, in principle, allow the maximum efficiency in a simple cycle without the regeneration of heat [4], the practical use of massive salt is hindered by several factors:

(a) substantial increase in the volume of the solid phase during the formation of the complex (it may attain 3–4 times for complexes with ammonia);

(b) hysteresis in the reaction (1), as a result of which the decomposition of the complex may occur at a much higher temperature than its formation;

(c) low rate of the reaction (1) due to the undeveloped reaction surface and/or the formation of a new phase on the salt surface, the diffusion of the gas through which is hindered;

(d) corrosion activity of salts and complexes in contact with metallic parts of a CHP.

New two-components sorbents of ammonia [5–23] and water [24–49] were proposed to overcome these difficulties and to improve heat transfer; the microcrystallites of active salt in these sorbents were placed on the exterior or interior surface of a less active component — the matrix used as the dispersion agent and contributing to the improvement of heat ad mass transfer in the sorbent layer.

Below, we give data on new composite water and ammonia sorbents and demonstrate the possibility of "constructing" their sorption properties intentionally by varying the composition, the size of the host-matrix pores, and synthesis conditions. In closing, we consider the applications of the new materials in adsorption refrigerating devices.

[a]G. K. Boreskov Institute of Catalysis, Siberian Branch of the Russian Academy of Sciences. 5 Akad. Lavrentiev Ave., Novosibirsk, 630090, Russia; email: aristov@catalysis.nsk.su; [b]A. V. Luikov Heat and Mass Transfer Institute, National Academy of Sciences of Belarus, 15 P. Brovka Str., Minsk, 220072, Belarus; email: lvasil@hmti.ac.by. Translated from Inzhenerno-Fizicheskii Zhurnal, Vol. 79, No. 6, pp. 160–175, November–December, 2006. Original article submitted April 18, 2006.

 1062-0125/06/7906-1214

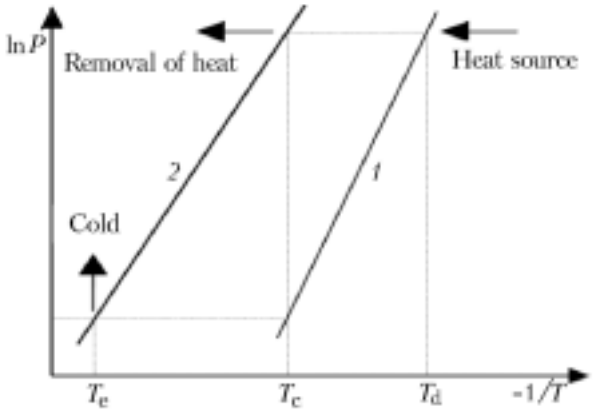

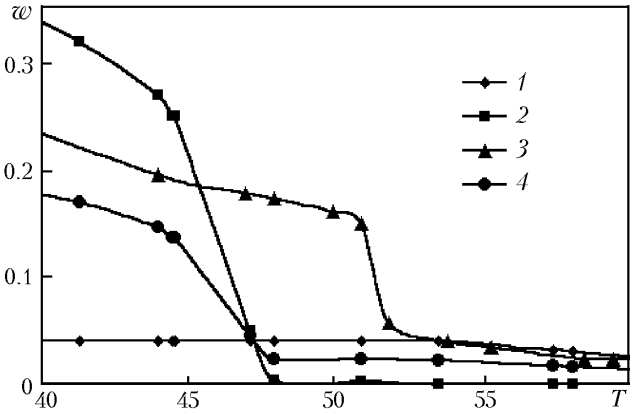

Fig. 1. Thermodynamic cycle of a CHP: 1) monovariant equilibrium; 2) evaporation and condensation of a pure working fluid.

Fig. 2. Isobars of steam sorption by a silica gel with a pore size of 12 nm (1), a massive $Ca(NO_3)_2$ (2), and a selective water sorbent (12 nm) (3) and a linear combination of sorption properties of the silica gel and the massive $Ca(NO_3)_2$ (4) [28]. T, ^oC; w, g/g.

Composite Sorbents of Steam. The regularities of formation and decomposition of hydrates of different salts (halogenides, sulfates, and nitrates), dispersed in the pores of aluminum oxide, silica gel, coal, and others (so-called selective water sorbents (SWSs)), have been investigated in many works, and the basic conclusions have been presented in [24–27].

1. *The adsorption of water by a composite is not a linear superposition of the adsorption by a salt and a matrix, i.e., synergism of properties is observed.* This is illustrated by Fig. 2 [28] which gives the isobars of sorption of steam by massive calcium nitrate or silica gel KSS-2 (average pore diameter 12 nm). For the sake of comparison we show curve 4 calculated as a linear combination of these isobars with the corresponding weight contributions: $m_\Sigma(T) = \alpha \cdot m\mathrm{Ca(NO_3)_2}(T) + (1-\alpha)\cdot m\mathrm{SiO_2}(T)$, where $m\mathrm{Ca(NO_3)_2}(T)$ and $m\mathrm{SiO_2}(T)$ are the amounts of water (g) absorbed, at temperature T, by 1 g of the massive $Ca(NO_3)_2$ and 1 g of the silica gel respectively and the experimental isobar for the selective water sorbent composite (12 nm), i.e., the silica gel KSS-2 modified by calcium chloride. For a pure silica gel the sorption smoothly grows with decrease in the temperature and attains 0.04 g H_2O/g. Unlike this, water is absorbed by the massive salt in steps: by formation of the salt dihydrate

$$\mathrm{Ca(NO_3)_2 + 2H_2O \leftrightarrow Ca(NO_3)_2 \cdot 2H_2O}\ . \qquad (2)$$

There are three phases (anhydrous salt, its crystalline hydrate, and steam) and two components (salt and water) in the system. According to the Gibbs phase rule, the number of degrees of freedom of an equilibrium system $\nu = k + 2 - f$, where f is the number of phases, is generally equal to unity in this case, i.e., the system is monovariant. This means that we can vary only one parameter of the two external parameters (T and P_{H_2O}) along the equilibrium curve. If, e.g., the pressure is fixed (as in our experiments), the variance of the $\nu = k + 1 - f$ system becomes equal to zero and the transition from the anhydrous salt to a dihydrate is stepwise at a certain threshold temperature. At P = 17 mbar, this temperature is equal to 45 ± 2^oC (Fig. 2), which corresponds to a relative humidity of 18%.

2. *The reaction of hydrate formation shifts to the region of higher temperatures with decrease in the size of the host-matrix pores.* Indeed, as the size of the host-matrix pores decreases, the temperature of transition between the anhydrous salt and its crystalline dihydrate shifts to the region of higher temperatures or, in other words, to the region of lower relative humidities (from 18 to 9–11%) (Fig. 3). Thus, the dispersion of the salt to a nanosize increases its capacity for absorbing water.

In addition to the shift to the region of higher temperatures, the transition region becomes broadened: its length is 5–7 and $12–15^oC$ respectively for the composite selective water sorbents (15 nm) and selective water sorbents (6 nm) (Fig. 3). In our opinion, this points to the inhomogeneity of the properties of the nanocrystallites of the

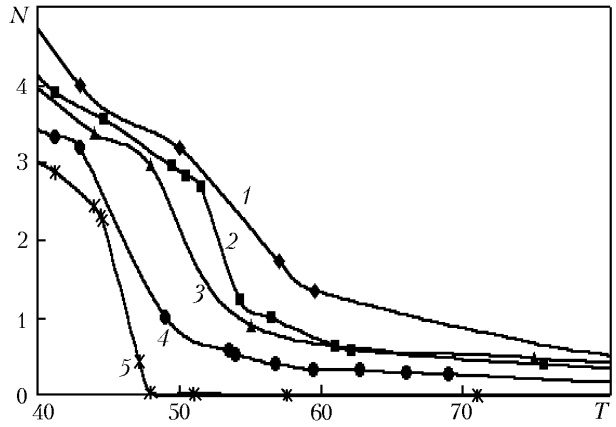

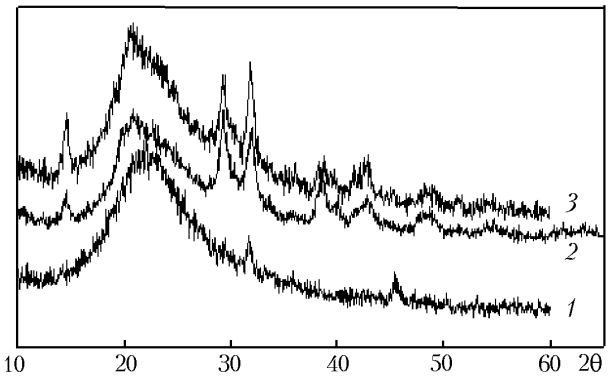

Fig. 3. Isobars of steam sorption by composites synthesized based on silica gels with different pore size; 1) 6; 2) 10; 3) 12; 4) 15 nm; 5) massive calcium nitrate [28]. *N*, mole of H_2O/mole of salt, *T*, °C.

Fig. 4. X-ray photographs of the samples: 1) $CaCl_2$ (33.7%)/SiO_2; 2) $CaCl_2$ (23.3%)/SiO_2; 3) $CaCl_2$ (10.7%)/SiO_2. θ, deg.

TABLE 1. Relative Humidity for Which the Transitions between the Hydrates Considered in Massive and Dispersed (in Pores with an Average Diameter of 15 nm) States Occur (P_{H_2O} = 15–20 mbar) [27]

Salt	Transition	Massive state	Dispersed state
Na_2SO_4	1 => 7	0.80	0.5—0.6
	7 => 10	0.91	—
Na_2HPO_4	0 => 2	0.37—0.39	—
	2 =>7	0.52—0.57	—
$Ca(NO_3)_2$	0 => 2	0.21—0.23	0.15—0.19
$MgSO_4$	0 => 1	0.03	0.001—0.003
	1 => 2	0.05—0.06	0.003—0.01
	2 => 4	0.15—0.17	—
	4 => 6	0.24—0.30	—
$CaCl_2$	0 => 1/3	< 0.01	—
	1/3 => 2	0.04—0.05	0.03—0.04
	2 => 4	0.16—0.18	0.12—0.14
LiBr	0 => 1	0.01	0.01
	1 => 2	0.04—0.05	0.02—0.03
LiCl	0 => 1	0.09—0.12	0.04—0.05
	1 => 2	0.12—0.13	0.06—0.09

salt dispersed in the pores of the silica gel, so that, for different crystallites, the transition (2) follows a monovariant course but at different temperatures, shifting, on the whole, to the region of temperatures higher than those in the case of a massive salt. The reason for this inhomogeneity can be both the size distribution of the crystallites of the dispersed salt and the chemical interaction of the salt with the matrix.

The found phenomenon of the equilibrium shift in the reaction of formation of salt hydrates, when the salt is placed in the host-matrix pores, is general in character (see Table 1) and can be used for nanoconstruction of new composite sorbents with properties optimum for a prescribed CHP (AHP) cycle.

3. *For the salt in the pores, hysteresis decreases or disappears.* It has turned out that hysteresis is observed in the region of the transition (2) for the massive $Ca(NO_3)_2$ and the selective water sorbent composite (12 nm); the difference between the curves of formation (sorption) and decomposition (desorption) is much smaller for the salt in

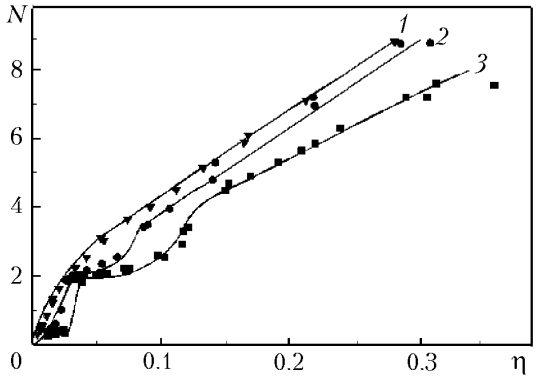

Fig. 5. Isotherms of vapor sorption by the systems: 1) $CaCl_2$ (10.7%)/SiO_2; 2) $CaCl_2$ (23.3%)/SiO_2; 3) $CaCl_2$ (33.7%)/SiO_2 [29].

the pores than that for the massive salt (Fig. 3). This hysteresis can be due to the kinetic difficulties in fitting of water molecules into the crystal lattice of the salt. A decrease in the hysteresis can result from both the dispersion of the salt to a nanosize, which is accompanied by the increase in the number of defects, and its interaction with the carrier surface. No sorption hysteresis was observed for the solution in the silica-gel pores.

4. *The salt in the pores forms two phases: a crystalline phase and an amorphous phase.* They qualitatively differ in the character of water absorption. This, the phase composition of composite sorbents "calcium chloride in a mesoporous silica gel" with different contents of salt has been investigated in [29] by the methods of differentiating solution and x-ray phase analysis. The sorption equilibrium of the composite sorbents with the steam was studied by the thermogravimetric method in the temperature interval 20–200^{o}C at a steam pressure of 10–50 mbar. It has been shown that, as a consequence of the interaction of calcium chloride with the silica-gel surface, the salt in the pores forms two phases (Fig. 4): a bulk crystalline phase and a surface x-ray amorphous phase. Their relation is dependent on the content of the salt in the composite: the fraction of the crystalline phase grows with concentration of the salt. The sorption equilibrium of the composite sorbents with the steam is also dependent on the relation of these phases. In sorbents with a high content of salt (e.g., 33.7%), the salt is predominantly in the crystalline phase; in sorption of the steam, crystalline salt di- and tetrahydrates are formed in the pores by the reactions

$$CaCl_2 + 2H_2O \leftrightarrow CaCl_2 \cdot 2H_2O\,, \tag{3}$$

$$CaCl_2 \cdot 2H_2O + 2H_2O \leftrightarrow CaCl_2 \cdot 4H_2O\,. \tag{4}$$

The equilibrium of these reactions is monovariant, so that the sorption changes in steps at a relative pressure of 0.03–0.04 and 0.12–0.14 (Fig. 5). In sorbents with a low content of salt (10.7%), it is in the pores in the x-ray amorphous state. As a result, the composition of the hydrated phase varies continuously (Fig. 5), which is typical of solutions of salts or crystalline hydrates with a vacancy structure. When the content of salt is intermediate, we observe a transient behavior; the transitions in the reactions (3) and (4) shift to the region of lower relative pressures (Fig. 5). We can also efficiently change the relation between the crystalline and amorphous phases, varying the pH of the impregnating solution and the calcination temperature of the composite [30–32].

Generalization of the results of investigations of more than 30 composite sorbents enables us to infer that the sorption properties of a composite can intentionally be varied within wide limits by selecting the chemical nature of the salt and the matrix and the size of the matrix pores and by varying the synthesis conditions: the concentration and pH of the impregnating solution and the calcination temperature [24–27].

Composite Sorbents of Ammonia. In this section, we do not consider the large series of works on composite ammonia sorbents that represent *a mechanical mixture* of an active salt with an inactive component (usually expanded graphite, a neutral carbon fiber) [5, 6, 21–23, 33–35]. This component is primarily used for organization of the transfer of heat to the salt and partially compensates for the change in the salt volume during the reaction (1). The emphasis will be on composites in which the salt is to be found on the surface and in the pores located on the surface of a

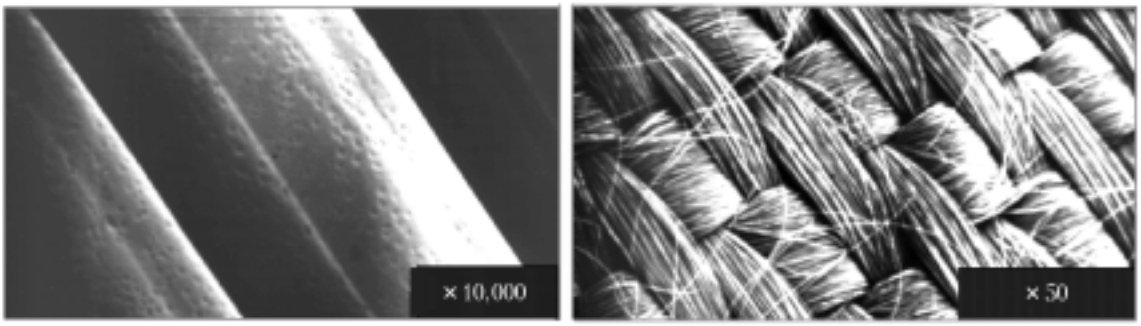

Fig. 6. Electron-microscopic photographs of an "AUTM busofite" activated carbon fiber.

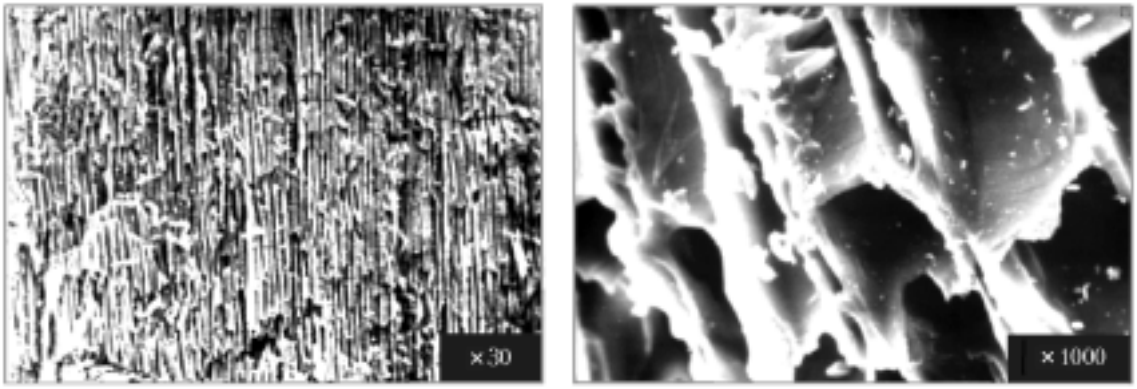

Fig. 7. Electron-microscopic photographs of DAU activated carbon.

host matrix (*active carbon fiber*), interacting with its exterior surface. Unlike the above water sorbents based on inorganic matrices, for ammonia absorption we used salt micro- and nanocrystals deposited on the surface of the active carbon fiber. Thus, we realized the possibility of using the physical adsorption of active carbon fiber and the chemical reaction of interaction of ammonia with the salt micro- and nanocrystals in one volume of the materials in one cycle. These were nonwoven materials based on the activated carbon fiber busofite [7–20] and manufactured from microfibers with micropores on the surface, or activated carbon produced from coconut shell [36], or activated charcoal.

Composites based on busofite in which micropores on the fiber surface made the main contribution to the absorption of ammonia, whereas macropores between the fibers contributed to the improvement of the process of mass exchange in diffusion of its vapor and allowed a convective ammonia flow by filtration of the vapor between the fibers, are the most extensively studied at present. Additionally activated fiber sorbents were used further for deposition on their surface (impregnation) of calcium, barium, manganese, and nickel chlorides. Since the microcrystals of metal chloride are quite uniformly distributed on the surface of carbon fibers, this prevents the process of single-crystallization" of the substance and solves the problem of change in the chloride volume in the adsorption and desorption of ammonia molecules. The free space between the fibers efficiently "absorbs" the volume expansion of a salt microcrystal in adsorption and keeps the volume virtually constant after multiple repetition of the cycles. Finally, the thermal conductivity of the composite increases; it is primarily determined by the thermal conductivity of the carbon fiber (activated carbon), which is equal to 0.2–0.4 W/(m·K). The production of a composite is concluded with the stage of molding (pressing), in the process of which the mass-size characteristics are improved. Figures 6 and 7 show photographs of the activated carbon fiber busofite and activated charcoal DAU, taken with an electron microscope.

Figure 8 gives the isotherms (obtained experimentally) of NH_3 adsorption on a modified busofite carbon fiber (after its add activation). The photographs of the composite material "AUTM-055 busofite–$CaCl_2$" are shown in Fig. 9. The arrangement of the salt crystallites on the fiber surface is pronounced in them.

From Figs 10–12, it is clear that the first NH_3 molecules are absorbed virtually in vacuum in the temperature range investigated. Next, as the pressure grows, we have successive reactions to form $CaCl_2{\cdot}4NH_3$ and $CaCl_2{\cdot}8NH_3$

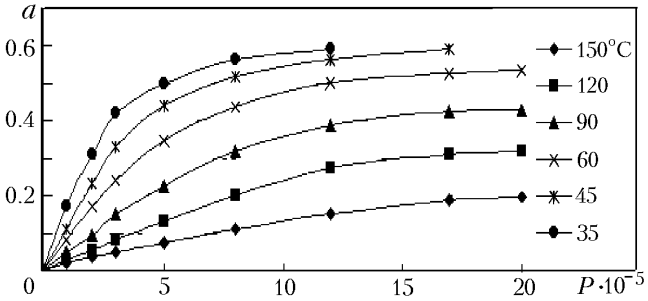

Fig. 8. Isotherms of ammonia sorption by a modified carbon fiber (after add activation); the sorbent temperature is 35–150°C. *P*, Pa; *a*, kg/kg.

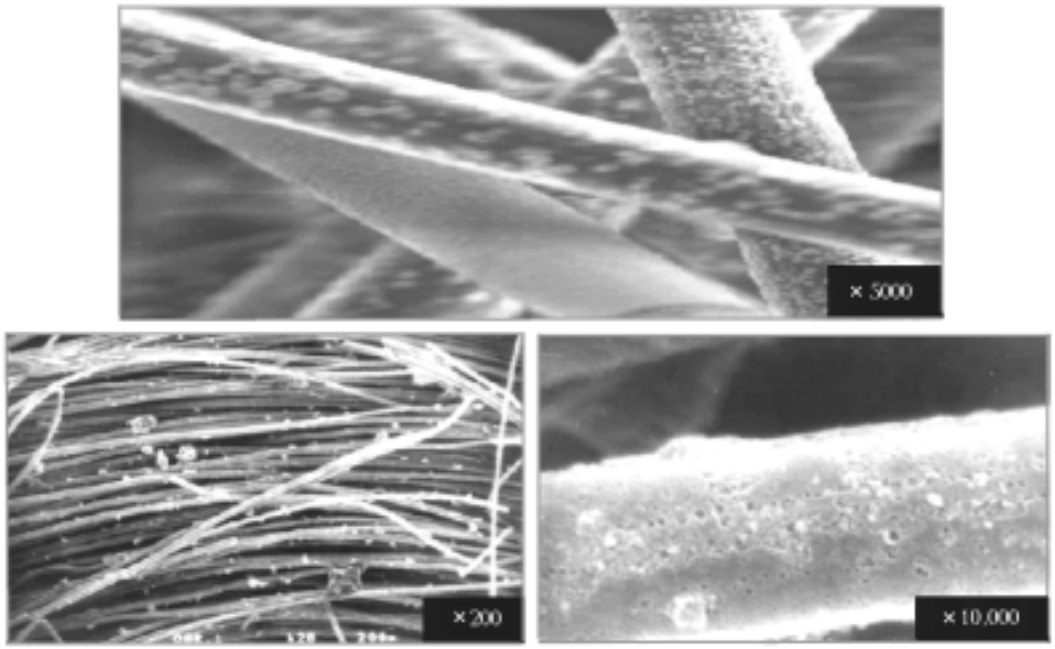

Fig. 9. Fibers of the activated carbon "busofite with $CaCl_2$ microcrystals on the surface."

complexes. Here, whereas the transition to octoammoniate is virtually not noticeable for 20°C, at 40°C, the pressure difference is significant now and is 50 kPa. Figure 12 gives the isotherms of chemical and physical sorption of ammonia on calcium chloride and carbon fiber, multiplied by the corresponding mass factor $\chi_1 = 0.32$ and $\chi_2 = 0.68$. The factor expresses the mass (weight) fraction of a given sorbent in the composite material. It is seen that the sum of these two plots of the physical and chemical sorption for each of the temperatures at which the experiments were conducted (20 and 40°C) results in the isotherms of ammonia sorption on the "AUTM-055 busofite–$CaCl_2$" compound.

The processes of physical and chemical sorption of ammonia are simultaneous, which explains the behavior of the isotherms on the initial portion ("steps" at $P/P_s < 0.1$). The presence of two mechanisms of sorption ensures the high adsorbability of the material produced. The developed procedure of synthesis of adsorbents ensures a uniform distribution of the microcrystallites of metal chlorides between the carbon fibers, which prevents the process of "single-crystallization" of the substance and solves the problem of change in the chloride volume in the adsorption and desorption of NH_3 molecules. The free space between the fibers efficiently "absorbs" the volume expansion of a salt crystal in adsorption and, as the investigations have shown, the busofite–metal chloride composite holds a virtually constant volume after multiple repetition of adsorption and desorption cycles.

Analogously to [7–20], we arrive at the following conclusions:

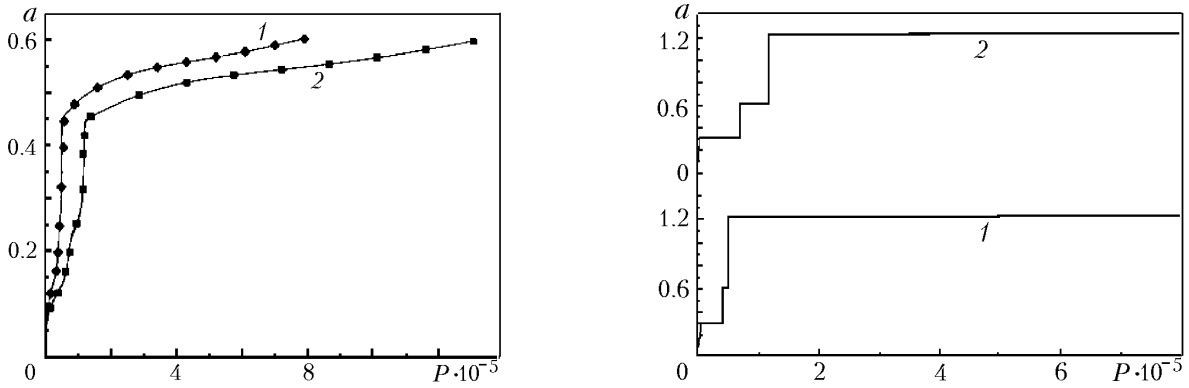

Fig. 10. Experimental isotherms of ammonia adsorption on the "busofite + $CaCl_2$" composite for temperatures of 20 (1) and 40°C (2). *P*, Pa; *a*, kg/kg.

Fig. 11. Isotherms of chemical sorption of ammonia on $CaCl_2$ for temperatures of 20 (1) and 40°C (2). *P*, Pa; *a*, kg/kg.

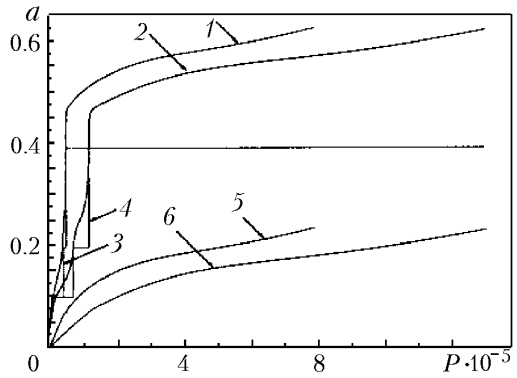

Fig. 12. Isotherms of ammonia adsorption of the compound "AUTM-055 busofite + $CaCl_2$" (1) 20, 2) 40°C), isotherms of NH_3 chemisorption of $CaCl_2$, multiplied by χ_1 (3) 20, 4) 20°C), isotherms of NH_3 adsorption on AUTM-055 busofite, multiplied by χ_2 (5) 20, 6) 40°C). *P*, Pa; *a*, kg/kg.

1. The arrangement of the microcrystals of metal salts on the surface of the active carbon fibers of busofite substantially increases the surface of their interaction with the ammonia vapor and accelerates the process of sorption; also, it substantially increases the sorptive capacity of the sorbent.

2. Since the active carbon fibers are a "fast" sorbent, the ammonia vapor is sorbed first by busofite (micropores on the fiber surface "operate" during the first 3–5 min), and next is the sorption by the salt microcrystals (when the necessary synthesis temperature, i.e., the plateau, is attained). This process is clearly seen in analyzing the isotherms of ammonia sorption by the composite.

3. In the process of sorption of the ammonia vapor, there is mass exchange between the active carbon and the microcrystals of metal salt, which can take part of the ammonia molecules from busofite in the process of the reaction reaching the plateau, allowing the additional adsorption of the ammonia molecules by the active carbon late in sorption.

4. The salt on the carbon-fiber surface and in micropores forms two phases: a crystalline bulk phase (microcrystals) and an amorphous surface phase which qualitatively differ in the character of ammonia absorption, which is consistent with the behavior of the salt as part of the composites.

The main difference of "salt on fiber" sorbents from selective water sorbents is that their sorption properties are a linear superposition of the properties of the salt and the matrix, and the temperatures of formation of ammoniates in the massive and dispersed states coincide. Accordingly we can affect the properties of a composite, changing the

chemical nature of the salt and the matrix and their relative contents. The salt in these composites is to be found on the exterior carbon surface (or in *macropores*), which facilitates the reagent (ammonia) access to them.

It is noteworthy that, when active salts (calcium and barium chlorides) are placed in the pores of inorganic matrices (aluminum oxide and vermiculite), we obtain composites with sorption properties that are no longer the superposition of the properties of the matrix and the salt [37, 38]. Thus, a decrease in the enthalpy and entropy of the reaction (1) for a dispersed salt and a shift of the transition between salt complexes with four and eight NH_3 molecules to the region of higher pressures have been found [37].

Thus, the series of systematic investigations of the properties of "salt in the matrix" and "salt on fiber" composites has shown that the placement of the salt in the pores or the arrangement of microcrystals on the fiber surface enables us to eliminate or at least to diminish the influence of negative factors characteristic of CHPs with a massive salt, since it: 1) accelerates sorption, 2) improves the total sorptive capacity, 3) makes the hysteresis narrower, 4) partially compensates for the expansion of the salt due to the void volume, and 5) eliminates the contact of corrosive substances with the walls of the plant due to their encapsulation in the pores.

Another important advantage of these composites is in the possibility of controlling their sorption properties by changing their composition and synthesis conditions, which enables us, in principle, to produce a material optimum for a specific CHP (AHP) cycle [27].

Laboratory prototypes of adsorption thermal plants (heat pumps, refrigerators, and systems for storage and transportation of gases at a low pressure in the sorbed state) operate on the basis of the composite sorbents studied, and they show better characteristics than in the case where regular one-component sorbents are used [39–46, 50–52].

Use of New Composite Sorbents for Obtaining Cold and Heat. The behavior of a laboratory prototype of an AHP for obtaining water with temperature $T_e = 10^oC$ with the use of a low-temperature heat source and a "water–SWS-1K composite" working pair has experimentally been investigated in [41–43]. The adsorbent represented a mesoporous KSK silica gel modified by calcium chloride whose content amounted to 33.7% wt.%. The properties of this material had been studied earlier [29, 31, 47, 48] in detail, which made it possible to select it for this application. Indeed, the salt tetrahydrate is completely decomposed in the pores at the relative pressure $\eta = 0.12$ (Fig. 5); consequently, a temperature of 80^oC is sufficient for complete decomposition at the condenser temperature $T_c = 35^oC$. Such a low decomposition temperature enables us to use, as the AHP motive force, heat sources with a low temperature potential, e.g., heat from the cooling system of different engines, from plane solar-energy receivers, from geothermal water, etc.

Tests of the laboratory AHP prototype made it possible to evaluate the coefficient of performance of a refrigerating machine (COP), whereas a comparison of the results obtained for two adsorber structures — with a granular adsorbent bed [41–43] and a compact bed [42, 46] — enabled us to propose recommendations on increasing the COP and the specific refrigerating power of AHPs.

The first adsorber/heat exchanger consisted of eight series-connected finned tubes made of stainless steel. The entire space between the plates and the tubes was filled with 0.8–1.6 mm granules (mass 1.1 kg) of the SWS-1K adsorbent. The sorbent was prepared according to the standard procedure by impregnating the mesoporous KSK silica gel with the aqueous solution of calcium chloride [47]. The characteristics of the first adsorber/heat exchanger with a granular bed are given below:

Number of tubes	8
Tube length, mm	200
Distance between the fins, mm	7
Fin thickness, mm	0.4
Heat-exchange surface, m^2	0.4
Metal/adsorbent mass ratio	3

The second adsorber/heat exchanger consisted of 16 parallel-connected aluminum finned tubes. The space between the plates was filled with paste containing SWS-1K (33.5 wt./% of salt) and a binder. The paste was dried at a temperature of 200^oC until the weight loss stopped. The characteristics of the second adsorber/heat exchanger with a compact bed are given below:

Metal mass, kg	6.08
Sorbent mass, kg	1.75

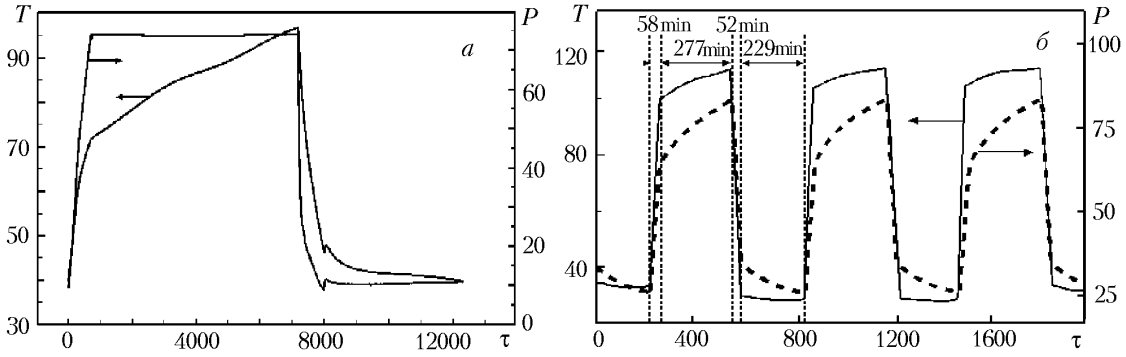

Fig. 13. Evolution of temperature and pressure in the adsorption cooler [41]: a) granular bed; b) consolidated sorbent bed. T, ^{o}C; P, mbar; τ, min.

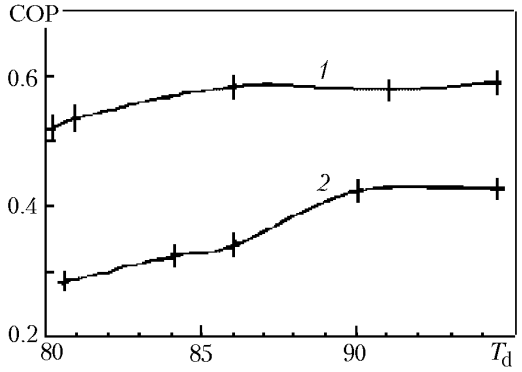

Fig. 14. Efficiency of the adsorption cooler with a granular sorbent bed vs. desorption temperature at different condenser temperatures: 1) 35; 2) 40^{o}C. T, ^{o}C.

Volume, liters	8.6
Length, m	0.56
Distance between the fins, mm	7
Tube diameter, mm	11
Number of tubes	16
Heat-exchanger surface, m^2	~1.7
Sorbent/metal mass ratio	0.29

Most of the experiments were conducted at T_c = 35 and 40^{o}C and T_e = 10^{o}C typical of adsorption air-conditioning systems. The desorption temperature was 80–100^{o}C. The COP was calculated as the ratio of heat absorbed in the evaporator to the total quantity of heat supplied to the system from the external source in a working cycle [41].

Below, we present the evolutions of temperature and pressure in the adsorption cooler with granular (Fig. 13a) and consolidated sorbent beds (Fig. 13b).

The calculated and experimental cycles of the device under study, which are presented on the Clapeyron diagram, turned out to be similar [41]. The time evolution of temperature (average over the sorbent volume) and pressure during the working cycle under study shows that the cycle is much shorter for the case of a compact sorbent bed that that for a granular bed (10–15 and 160 min respectively, Fig. 13). The isosteric stages of heating and cooling were rapid, whereas isobaric desorption taking 5 and 90 min was the slowest process. Accordingly the average refrigerating powers were 150–200 and 25–30 W/kg, and the net specific power in the adsorption stage was 350–400 and 50–60 W/kg. The low specific power in the case of a granular adsorbent bed is attributable to the low heat-transfer efficiency related to both the low thermal conductivity of the granular bed and the high resistance at the sorbent–heat-exchanger boundary. Heat transfer was substantially improved, when the adsorbent was prepared in the form of a compact bed integrated with the heat-exchanger wall, with the result that the specific power increased 5–6 times and attained values (350–400 W/kg) that could be of real interest, i.e., for air conditioning in the interior of an automobile.

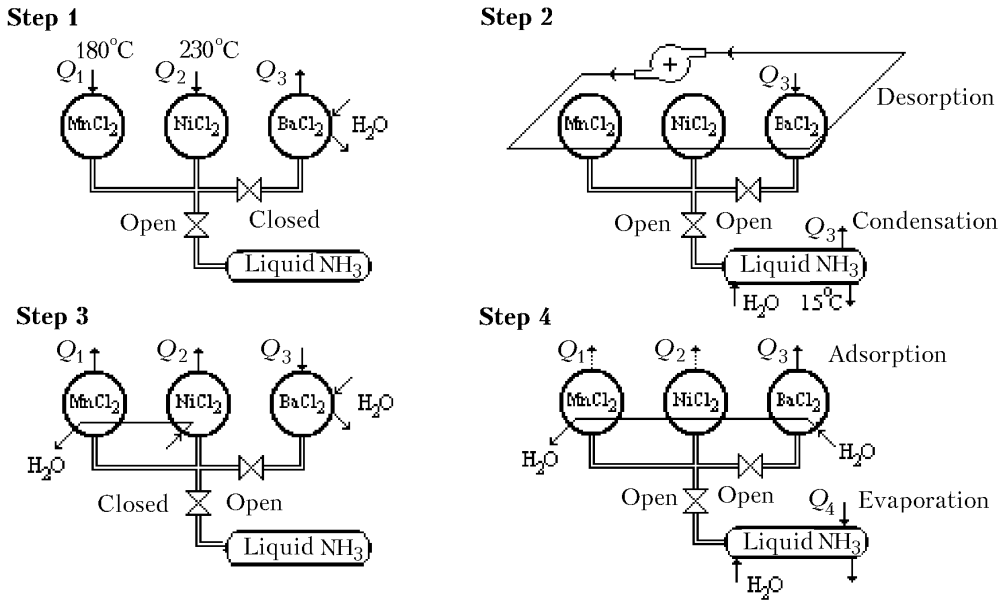

Fig. 15. Diagram of a three-cascade heat pump.

The efficiency of the refrigerating device was calculated from experimental data at two condenser temperatures (Fig. 14). It turned out that the efficiency increases with desorption temperature up to T_d = 85–90°C, after which it attains 0.59 ± 0.05 (at T_c = 35°C) and 0.42 ± 0.05 (at T_c = 40°C) for the granular bed. The high efficiency obtained opens up possibilities for further use of the adsorbent in adsorption refrigerators; the more so since:

(a) it is the real efficiency of the device tested that allows for the total heat loss, the heat capacity of inert metallic parts of the device, and the efficiency of all heat exchangers. These factors have not completely been optimized in the device tested, and we hope to improve this output characteristic in the future. To evaluate the possibility of improvement, we calculate the maximum theoretical efficiency of a refrigerating cycle without regeneration as

$$\mathrm{COP}_{\max} = (T_e/T_d)(T_d - T_c)/(T_c - T_e)\,,$$

at T_c = 35, T_e = 10, and T_d = 80°C, it is equal to 1.44, i.e., exceeds the value obtained in our experiments by nearly 2.5 times;

(b) this laboratory prototype incorporated one adsorber; there was no recuperation of heat in it. In a multiadsorber version of refrigerator, one can organize the transfer of heat between the adsorbers thus increasing the COP. Evaluation of the maximum quantity of recuperated heat according to the procedure of [49] has shown that COP = 0.83 can be attained in the case of ideal regeneration [42].

We note that a value of the efficiency of 0.6 obtained experimentally is fairly high and is of practical interest now. This efficiency is mainly due to the good sorption properties of the SWS-1K material and primarily to the fact that a large amount of water (e.g., 14 wt.% at T_c = 35°C, which is just similar to the transition between calcium-chloride di- and tetrahydrates) is formed between the evaporator and the condenser in the working cycle. Accordingly the evaporation of this water yields a high value of energy adsorbed in the evaporator in a cycle; this value is equal to 280 kJ/kg. At a higher condenser temperature, the value of Δw decreases, which accordingly leads to a reduction in the efficiency.

Another important result of the tests is that the properties of the composite remain constant during 1000 complete working cycles [46]. An analysis of the material after 1000 cycles has shown that the granules of the substance do not disintegrate and no dust is formed. Also, no traces of calcium chloride in the condensed water and on the interior surface of the plant were found. This proves the high hydrothermal stability of the composite and confirms the possibility of its practical use in sorption technologies of air conditioning.

Ammonia-Based AHPs are the Alternative of Water-Based AHPs. During the experimental investigations of the properties of sorbents, carried out at the Heat and Mass Transfer Institute of the National Academy of Sciences

Fig. 16. Heat pump with three adsorbers and a condenser/evaporator, intended for use in a system of energy trigeneration (production of electricity, heat, and cold) and operating with two pairs of adsorbers in antiphase.

of Belarus [10–16], 128 g of activated carbon fabric were in the adsorber. The adsorbability of carbon fibers with calcium-chloride microcrystals was 0.61 kg/kg at 20°C and a pressure of 800 kPa; the total amount of the ammonia absorbed by the compound was 227.1 g, of which 85 g was adsorbed by the activated carbon fiber and 142.1 g was adsorbed by calcium chloride.

A three-cascade AHP developed and tested at the Heat and Mass Transfer Institute of the National Academy of Sciences of Belarus (Fig. 15 and 16) ensures the regime of continuous heat and cold supply in the presence of two independent refrigerating sources. Waste gases of the diesel engine or its liquid-coolant loop are used as the power supply of the heat pump. Under laboratory conditions, electricity is used for heating of sorbents. A typical example of the employment of such a trigeneration system is the supply of dairy farms with power, heat, and cold (electricity for power supply of milking units and lighting, heat for hot water supply, and cold for cooling of milk).

The heat pump incorporates a high-temperature adsorber (activated carbon fiber impregnated with $NiCl_2/NH_3$), a medium-temperature adsorber (activated carbon fiber impregnated with $MnCl_2/NH_3$), a low-temperature adsorber — a refrigerator (activated carbon fiber impregnated with $BaCl_2/NH_3$), and an evaporator/condenser. An intensifier of heat transfer in the form of a porous coating is located in the evaporator/condenser to improve the evaporation of the liquid coolant. The heat pump has two sources of cold operating separately — the low-temperature $BaCl_2/NH_3$ adsorber and the condenser/evaporator — and is made in the form of two prototypes.

In the first, simpler prototype, three adsorbers of the pump simultaneously consume the energy of the waste gases from the internal combustion engine and the energy of the liquid cooling system of the engine for refrigeration.

Pump operation consists of two constituent cycles:

1. The adsorbers ($NiCl_2$, $MnCl_2$, and $BaCl_2$) initially are at room temperature and are heated, over a period τ_1, to a temperature of 230, 180, and 90°C respectively by the waste gases of the internal combustion engine or by the hot liquid from the cooling system of the engine. During the heating of the adsobers, we have the process of desorption of ammonia from the sorbent and the condensation of its vapor in the condenser/evaporator.

2. In the period of time τ_2, all the three adsorbers are cooled down to room temperature with water; the adsorption of the ammonia vapor by the sorbents, the evaporation of liquid ammonia in the evaporator, and decrease in its temperature down to −3°C, i.e., refrigeration, occur (Fig. 15).

The second, more complex prototype of a heat pump utilizes just the energy of the waste gases of the internal combustion engine. The energy removed by the liquid cooling system of the high-temperature $NiCl_2$ and medium-temperature $MnCl_2$ adsorbers is utilized in this prototype for heating of the low-temperature adsorber and for desorption of the ammonia vapor.

The heating of the $NiCl_2$ and $MnCl_2$ adsorbers to a temperature of 450°–500°C by the waste gases followed by their cooling by the liquid down to a temperature of 90°C makes it possible to transfer up to 1400 kJ to the low-temperature $BaCl_2$ and to carry out a two-stage process of ammonia desorption in it. We recall that the low-temperature adsorber contains a fast sorbent — busofite — on whose fiber surface there are the microcrystals of a slow

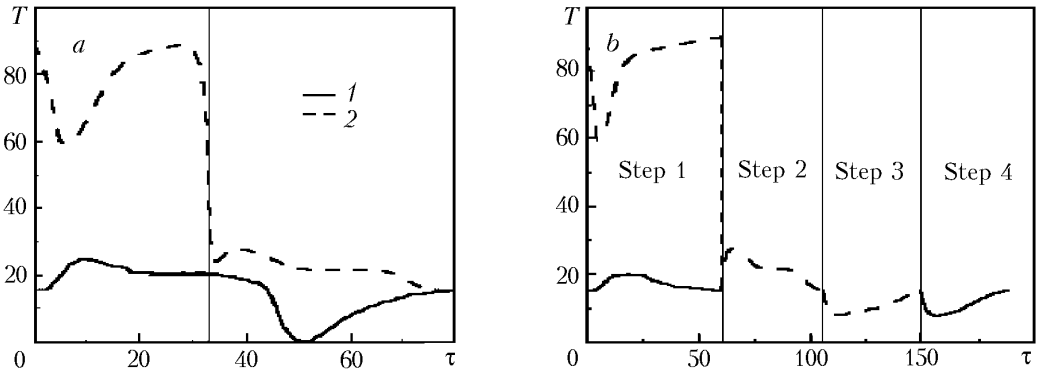

Fig. 17. Change in the water temperature at the outlet of the heat exchanger of the condenser/evaporator during the operating cycle of the heat pump for the first (a) and second (b) prototypes of the pump (the heat exchanger is in the low-temperature $BaCl_2$ adsorber): 1) desorption; 2) adsorption. T, ^oC; τ, min.

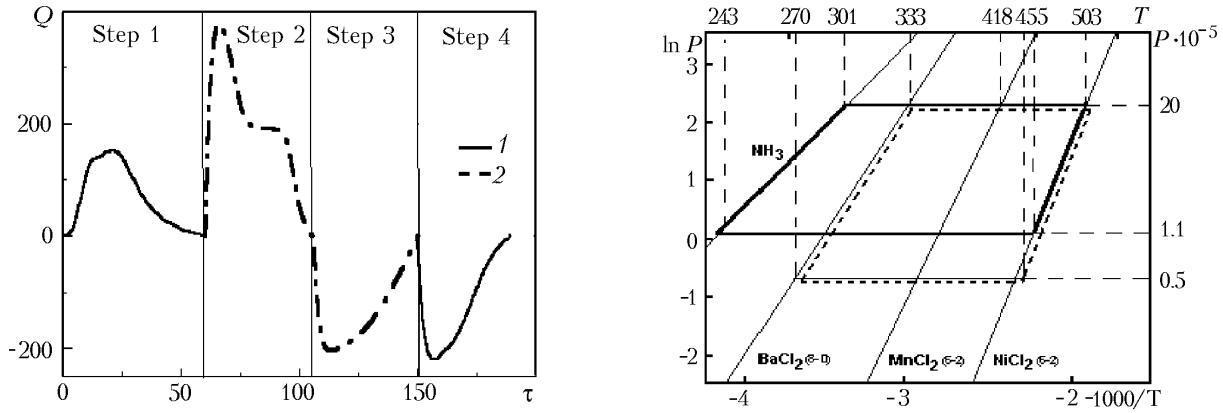

Fig. 18. Absorption ad release of heat in the condenser/evaporator (1) and the low-temperature $BaCl_2$ adsorber (2) as a function of time of the operating cycle of the heat pump (adsorption and desorption of the sorbent). Q, W; τ, min.

Fig. 19. Clapeyron diagram for the heat pump ($BaCl_2$, $MnCl_2$, $NiCl_2$ + activated carbon fiber busofite) with two sources of cold. P, Pa; T, K.

sorbent $BaCl_2$. The enthalpy of high-temperature adsorbers is expended in desorbing the ammonia vapor in the fast sorbent — active carbon fiber — with the subsequent condensation of the vapor in the condenser/evaporator. The desorption of the ammonia vapor from the microcrystals of the slow sorbent $BaCl_2$ occurs in the subsequent time interval, when the low-temperature $BaCl_2$ adsorber is already separated from the condenser/evaporator using a valve and is added to the high-temperature adsorbers. As they are subsequently cooled down, the process of suction of the ammonia vapor from the $BaCl_2$ microcrystals by the microcrystals of stronger sorbents $NiCl_2$ and $MnCl_2$ begins. In this manner the energy of the system of cooling of high-temperature adsorbers is utilized for refrigeration in the low-temperature adsorber (down to -30^oC).

In the second prototype of a heat pump, the process of refrigeration is carried out in four steps (time intervals $\tau_1 - \tau_4$):

1. *Time interval* τ_1. The $MnCl_2$ and $NiCl_2$ adsorbers are heated by the waste gases using heat pipes and the process of desorption of an ammonia vapor occurs; the ammonia vapor is condensed in the heat-pump's condenser and in the low-temperature $BaCl_2$ adsorber.

2. *Time interval* τ_2. The $MnCl_2$ and $NiCl_2$ adsorbers are separated from the condenser/evaporator using a valve and the process of their cooling begins. The cooling liquid having a temperature higher than 95^oC is fed to the

$BaCl_2$ adsorber. The sorbent is heated and the ammonia vapor is desorbed from the active carbon fiber, which is followed by its condensation in the condenser/evaporator.

Time interval τ_3. The process of cooling of all the three adsorbers to the ambient temperature is completed. The $BaCl_2$ adsorber is separated from the condenser/evaporator using a valve. The $MnCl_2$ and $NiCl_2$ adsorbers are connected with the $BaCl_2$ adsorber using another valve and the process of cooling of the $BaCl_2$ adsorber (the process of refrigeration) with desorption of the ammonia vapor begins, since the stronger sorbents in the $MnCl_2$ and $NiCl_2$ adsorbers take ammonia.

4. *Time interval* τ_4. The ammonia vapor begins to be adsorbed by all the three adsorbers; the cooling of the condenser/evaporator (refrigeration) with evaporation of the liquid ammonia in it occurs.

Figures 17 and 18 show the process of heating and cooling of the heat pump. The maximum heat-power input of the $MnCl_2$ and $NiCl_2$ adsorbers is 400 W per adsorber; here, 200 W of cold are produced in the evaporator (cooling of water circulating in it down to 10^oC).

An analysis of the Clapeyron diagram (Fig. 19) enables us to evaluate the operating efficiency of a heat pump with two sources of cold; it is equal to COP = 0.41 for the first prototype of the heat pump (three adsorbers + condenser/evaporator). For the second prototype of the heat pump, the coefficient of performance is equal to 0.62. A prototype of the heat pump is shown in Fig. 16.

Thus, the results of investigations of the new water and ammonia sorbents — "salt in a porous matrix" and "salt on fiber" composites — make it possible to "construct" their sorption properties by varying the composition, the size of the host-matrix pores, and synthesis conditions. Examples of using the new materials have been considered and prospects for using them in sorption refrigerating devices have been substantiated.

This work was carried out with financial support from the Russian Foundation for Basic Research (project Nos. 04-02-81028 and 05-02-16953), the Program of Integration Projects of the Siberian Branch of the Russian Academy of Sciences (project No. 102), and the Belarussian Republic Foundation for Basic Research (project No. T05BR-018).

NOTATION

a, adsorbability, kg/kg; COP, coefficient of performance of a refrigerating machine; *f*, number of phases; *k*, number of the components of the system; *m*, mass, kg; *n*, number of molecules in the compound; *N*, content of water in the crystalline hydrate; *P*, pressure, Pa (bar); *Q*, heat flux, W; *T*, temperature, K (^oC); *w*, absolute humidity, g/g; α, mass (weight) fraction of calcium nitrate in the composite; ν, variance; η, relative pressure; τ, time; θ, angle of scattering; χ, mass factor expressing the mass fraction of a given sorbent in the composite material. Subscripts: g, gaseous; sol, solid; e, evaporator; c, condenser; d, desorption; Σ, total; max, maximum; s, saturation.

REFERENCES

1. Adsorption refrigerator uses low-temperature waste heat, *Newletters*, No. 1, 7–9 (2000).
2. Q. Ma, R. Z. Wang, Y. J. Dai, and X. Q. Zhai, Performance analysis on a hybrid air-conditioning system in a green building, *Energy Buildings*, **38**, 447–453 (2006).
3. W. M. Raldow and W. E. Wentworth, Chemical heat pumps — a basic thermodynamic analysis, *Solar Energy*, **23**, 75–79 (1979).
4. V. E. Sharonov, M. M. Tokarev, and Yu. I. Aristov, Thermodynamics of chemical and thermal machines, *Abstr. 28th Siberian Thermophysical Seminar*, 12–14 October 2005, Novosibirsk (2005), pp. 236–237.
5. B. Spinner, Ammonia-based thermochemical transformers, *Heat Recovery Systems and CHP*, **13**, No. 4, 301–307 (1993).
6. S. Mauran, M. Lebrun, P. Prades, M. Moreau, B. Spinner, and C. Drapier, Active component and its use as reaction media, US Patent 5.283.219, Feb. 1 (1994).
7. L. L. Vasiliev, L. E. Kanonchik, F. F. Molodkin, and M. I. Rabetsky, Adsorption heat pump using carbon fiber/NH_3 and heat pipes, in: *Proc. 5th IEA Heat Pump Conf.*, 22–26 September 1996, Toronto, Canada (1996), pp. 35–43.

8. L. L. Vasiliev, D. A. Mishkinis, A. A. Antukh, and L. L. Vasiliev Jr., New solid sorption refrigerator, in: *Proc. 3rd Int. Seminar Heat Pipes*, *Heat Pumps*, *Refrigerators* [in Russian], 15–18 September 1997, Minsk, Belarus (1997), pp. 24–30.
9. L. Vasiliev, V. Babenko, and L. Kanonchik, Heat and mass transfer intensification in solid sorption systems, *J. Enhanced Heat Transfer* (*USA*), **5**, No. 2, 111–125 (1998).
10. L. L. Vasiliev, D. A. Mishkinis, A. A. Antukh, and L. L. Vasiliev Jr., Solar-gas solid sorption heat pump, *ISHPC*, in: *Proc. Int. Sorption Heat Pump Conf.*, 24–26 March 1999, Munich, Germany (1999), pp. 117–122.
11. L. L. Vasiliev, D. Nikanpour, A. A. Antukh, K. Snelson, L. L. Vasiliev Jr., and A. Lebru, Multisalt-carbon chemical cooler for space applications, *ISHPC*, in: *Proc. Int. Sorption Heat Pump Conf.*, 24–26 March 1999, Munich, Germany (1999), pp. 579–583.
12. L. L. Vasiliev, D. A. Mishkinis, A. A. Antuh, and L. L. Vasiliev Jr., A solar and electrical solid sorption refrigerator, *Int. J. Thermal Sci.*, **38**, 220–227 (1999).
13. L. L. Vasiliev, D. A. Mishkinis, A. A. Antukh, and L. L. Vasiliev Jr., Solar-gas refrigerators, in: *Proc. 7th Int. Symp. on Thermal Engineering and Sciences for Cold Regions*, *Advances in Thermal Engineering and Sciences for Cold Regions*, 12–14 July 2001, Seoul, Korea (2001), pp. 277–282.
14. L. L. Vasiliev, D. A. Mishkinis, A. A. Antuh, and L. L. Vasiliev Jr., Solar-gas solid sorption refrigerator, *Adsorption*, **7**, 149–161 (2001).
15. L. Vasiliev, D. Mishkinis, A. Antukh, A. Kulakov, and L. Vasiliev Jr., Multisalt-carbon portable resorption heat pump, *NATO ASI SERIES VOLUME: Low Temperature and Cryogenic Refrigeration — Fundamentals and Applications*, Altin Yunus–Cesme, 23 June 5–July 2002, Izmir, Turkey (2002), pp. 387–400.
16. L. L. Vasiliev, Solar sorption refrigerators with dual sources of energy, *ISHPC'02*, in: *Proc. Int. Sorption Heat Pump Conf.*, 24–27 September 2002, Shanghai, China (2002), pp. 26–33.
17. L. L. Vasiliev, Sorption machines with a heat pipe thermal control, *ISHPC'02*, in: *Proc. Int. Sorption Heat Pump Conf.*, 24–27 September 2002, Shanghai, China (2002), pp. 408–413.
18. L. L. Vasiliev, Solar sorption refrigerator, in: *Proc. 5th Minsk Int. Seminar Heat Pipes*, *Heat Pumps*, *Refrigerators* [in Russian], 8–11 September 2003, Minsk, Belarus (2003), pp. 364–379.
19. L. L. Vasiliev, L. L. Vasiliev Jr., A. A. Antukh, A. G. Kulakov, M. I. Rabetsky, and D. A. Mishkinis, Resorption heat pump, in: *Proc. 5th Minsk Int. Seminar Heat Pipes*, *Heat Pumps*, *Refrigerators* [in Russian], 8–11 September 2003, Minsk, Belarus (2003), pp. 450–460.
20. L. L. Vasiliev, D. A. Mishkinis, A. A. Antukh, A. G. Kulakov, and L. L. Vasiliev Jr., Resorption heat pumps, *Appl. Thermal Eng.*, **24**, 1893–1903 (2004).
21. Z. Aidom and M. Ternan, Salt impregnated carbon fibers as the reactive medium in a chemical heat pump: the $NH_3/CoCl_2$ system, *Appl. Thermal Eng.*, **22**, 1163–1173 (2002).
22. K. Fujioka, K. Hatanaka, and Yu. Hirata, Composite reactants of calcium chloride combined with functional carbon materials for chemical heat pumps, in: *Proc. 6th Int. Seminar Heat Pipes*, *Heat Pumps*, *Refrigerators*, 12–15 September 2005, Minsk, Belarus (2005), pp. 306–315 (2005).
23. L. W. Wang, R. Z. Wang, J. Y. Wu, K. Wang, and S. G. Wang, Compound adsorbent for adsorbing ice makers on fishing boats, *Int. J. Refrig.*, **27**, 401–408 (2004).
24. Yu. I. Aristov, *Thermochemical Storage of Energy: New Methods and Materials*, Abstract of Doctoral Dissertation (in Chemistry), Novosibirsk (2003).
25. M. M. Tokarev, *Composite Sorbents "Calcium Chloride in a Porous Matrix,"* Abstract of Candidate's Dissertation (in Chemistry), Novosibirsk (2003).
26. L. G. Gordeeva, *New Materials for Thermochemical Storage of Energy*, Author's Abstract of Candidate's Dissertation (in Chemistry), Novosibirsk (2000).
27. Yu. I. Aristov, An optimal sorbent for adsorption heat pumps: thermodynamic requirements and molecular design, in: *Proc. 6th Int. Seminar Heat Pipes*, *Heat Pumps*, *Refrigerators* [in Russian], 12–15 September 2005, Minsk, Belarus (2005), pp. 342–353.
28. I. A. Simonova and Yu. I. Aristov, Sorption properties of calcium nitrate dispersed in silica gel: influence of the pore size, *Zh. Fiz. Khim.*, **79**, No. 8, 1477–1481 (2005).

29. L. G. Gordeeva, I. S. Glaznev, V. V. Malakhov, and Yu. I. Aristov, Influence of the interaction of calcium chloride with the silica-gel surface on the phase composition and sorption properties of disperse salt, *Zh. Fiz. Khim.*, **77**, No. 11, 2019–2023 (2003).
30. L. G. Gordeeva, I. S. Glaznev, and Yu. I. Aristov, Water sorption by sodium, copper, and magnesium sulfates dispersed in the silica gel and aluminum oxide mesopores, *Zh. Fiz. Khim.*, **77**, No. 10, 1930–1935 (2003).
31. L. G. Gordeeva, A. V. Gubar', L. M. Plyasova, V. V. Malakhov, and Yu. I. Aristov, Composite sorbents of water "salt in the silica gel pores": influence of the interaction of the salt with the surface on the chemical and phase composition and sorption properties, *Kinet. Katal.*, **46**, No. 5, 780–786 (2005).
32. L. G. Gordeeva, E. V. Savchenko, I. S. Glaznev, V. V. Malakhov, and Yu. I. Aristov, Impact of phase composition on water adsorption on inorganic hybrides "salt/silica," *J. Colloid. Interface Sci.*, **17**, 341–348 (2006).
33. M. Balat and B. Spinner, Optimization of a chemical heat pump: energetic density and power, *Heat Recovery Systems and CHP*, **13**, 277–285 (1993).
34. B. Spinner and Ph. Touzain, Application of exfoliated graphite intercalation compounds in order to improve the performance of thermochemical energy conversion process, *Workshop Carbone*, Paris (1990), pp. 145–162.
35. K. Wang, J. Y. Wu, R. Z. Wang, and L. W. Wang, Composite adsorbent of $CaCl_2$ and expended graphite for adsorption ice makers on fishing boats, *Int. J. Refrig.*, **29**, 199–210 (2006).
36. R. Critoph, Properties of a hydrid adsorbents with ammonia refrigerant, in: *Proc. 3rd Int. Conf. on Heat Powered Cycles*, 11–13 October 2004, Larnaca, Cyprus, (2004), pp. 12–32.
37. V. E. Sharonov, J. V. Veselovskaya, and Yu. I. Aristov, Ammonia sorption on composites "$CaCl_2$ in inorganic host matrix": isosteric chart and its performance, *Int. J. Low Carbon Technol.*, **1**, No. 3, 191–200 (2006).
38. V. E. Sharonov, J. V. Veselovskaya, Yu. I. Aristov, Y. Zhong, and R. E. Critoph, New composite adsorbent of ammonia "$BaCl_2$ in vermiculite" for adsorptive cooling, in: *Proc. Int. Conf. on Heat Powered Cycles*, 11–14 September 2006, Newcastle (2006), pp. 135–142.
39. L. L. Vasil'ev, Prospects of application of heat pumps in the Republic of Belarus, in: *Heat Transfer–MIF-2004: 5th Minsk Int. Forum* [in Russian], 24–28 May 2004, Minsk (2004), pp. 96–97.
40. L. L. Vasiliev, A. G. Kulakov, A. A. Antukh, and L. L. Vasiliev Jr., Chemical heat pump, in: *Proc. 3rd Int. Conf. on Heat Powered Cycles*, 11–13 October 2004, Larnaca, Cyprus (2004), Paper No. 2209.
41. G. Restuccia, A. Freni, S. Vasta, and Yu. I. Aristov, Selective water sorbents for solid sorption chiller: experimental results and modelling, *Int. J. Refrig.*, **27**, No. 3, 284–293 (2004).
42. G. Restuccia, A. Freni, S. Vasta, M. M. Tokarev, and Yu. I. Aristov, Adsorption cooling machine based on the working pair "calcium chloride in silica gel–water," *Kholod. Tekh.*, No. 1, 2–6 (2005).
43. G. Restuccia, A. Freni, S. Vasta, M. M. Tokarev, and Yu. I. Aristov, Environmentally clean adsorption refrigerator based on the "$CaCl_2$ in silica gel" composite: a laboratory prototype, *Khim. Ustoich. Razv.*, **12**, 211–216 (2004).
44. Yu. I. Aristov, Certain environmental and economical aspects of the use of sorption heat facilities in Russia, *Khim. Ustoich. Razv.*, **12**, 751–755 (2004).
45. Yu. I. Aristov, G. Restuccia, G. Cacciola, and V. N. Parmon, A family of new working materials for solid sorption air conditioning systems, *Appl. Thermal Eng.*, **22**, No. 2, 191–204 (2002).
46. A. Freni, F. Russo, S. Vasta, M. Tokarev, Yu. Aristov, and G. Restuccia, An advanced solid sorption chiller using SWS-1L, *Appl. Thermal Eng.*, **26**, No. 16, 1807–1811 (2006).
47. Yu. I. Aristov, M. M. Tokarev, G. Cacciola, and G. Restuccia, Selective water sorbents for multiple applications: 1. $CaCl_2$ confined in mesopores of the silica gel: sorption properties, *React. Kinet. Cat. Lett.*, **59**, No. 2, 325–334.
48. Yu. I. Aristov, M. M. Tokarev, G. DiMarko, G. Cacciola, G. Restuccia, and V. N. Parmon, Vapor–condensed state and melting–solidification equilibria in the calcium chloride–water system dispersed in the silica-gel pores, *Zh. Fiz. Khim.*, **71**, No. 2, 253–258 (1997).
49. F. Meunier, Second law analysis of a solid adsorption heat pump operating on reversible cascade cycles: application to the zeolite–water pair, *Heat Recovery Systems*, **5**, 133–141 (1985).
50. A. A. Antukh, O. S. Filatova, A. G. Kulakov, and L. L. Vasiliev, Solid sorption coolers for tri-generation, *Int. J. Low Carbon Technol.*, Manchester University Press, 3/1, July 2006, pp. 28–35.

51. L. L. Vasiliev, L. E. Kanonchik, A. G. Kulakov, D. A. Mishkinis, A. M. Safonova, and N. K. Luneva, Activated carbon fiber composites for ammonia, methane and hydrogen adsorption, *Int. J. Low Carbon Technol.*, Manchester University Press, 2/1, April 2006, pp. 11–18.
52. L. L. Vasiliev, A. G. Kulakov, D. A. Mishkinis, A. M. Safonova, and N. K. Luneva, Activated carbon as a sorbent of gases, in: *Volume of Scientific Papers "Fullerenes and Fullerene-Like Structures"* [in Russian], A. V. Luikov Heat and Mass Transfer Institute of the National Academy of Sciences of Belarus, Minsk (2005), pp. 200–217.